Available online at www.sciencedirect.com

ScienceDirect

Journal of the Chinese Medical Association 81 (2018) 977−984

www.jcma-online.com

Original Article

Evaluating cerebral hemodynamics using quantitative digital subtraction angiography and flat-detector computed tomography perfusion imaging: A comparative study in patients with carotid stenosis

Liang-Wei Chen [a], Chung-Jung Lin [a,b], Wan-Yuo Guo [a,b,*], Sheng-Che Hung [a,b], Han-Jui Lee [a,b], Ko-Kung Chen [c], Feng-Chi Chang [a,b], Chao-Bao Luo [a,b], Wei-Fa Chu [a,b]

[a] *Department of Radiology, Taipei Veterans General Hospital, Taipei, Taiwan, ROC*
[b] *School of Medicine, National Yang-Ming University, Taipei, Taiwan, ROC*
[c] *Department of Biomedical Imaging and Radiological Sciences, National Yang-Ming University, Taipei, Taiwan, ROC*

Received September 27, 2017; accepted January 6, 2018

Abstract

Background: The efficacy of both quantitative digital subtraction angiography (QDSA) and flat-detector computed tomography perfusion (FD-CTP) is equivalent to that of magnetic resonance perfusion (MRP) in assessing perfusion deficits in carotid stenosis. This study evaluated the feasibility of using FD-CTP to monitor cerebral hemodynamics during carotid stenting.

Methods: Thirteen patients with extracranial carotid stenosis (>70%) were included. Both QDSA and two FD-CTP sessions were performed before and after carotid stenting. Cerebral circulation time (CCT) was defined as the difference between the time to peak (TTP) of the parietal vein and the cavernous internal carotid artery. For FD-CTP and MRP, regions of interest (ROIs) were placed in the middle cerebral artery territory at the basal ganglia level of both stenotic and contralateral hemispheres for measurement. The TTP ratio (rTTP) was defined as stenotic TTP divided by contralateral TTP; and ratio of cerebral blood volume (rCBV), ratio of mean transit time (rMTT), and ratio of cerebral blood flow (rCBF) were defined similarly. Both CCT and ratio perfusion parameters were compared during stenting.

Results: Before stenting, only rCBF ($r = 0.73$) and rTTP ($r = 0.58$) demonstrated correlations between FD-CTP and MRP; CCT correlated with only rMTT in MRP ($r = 0.69$). After stenting, only rCBF ($r = 0.56$) indicated a correlation between FD-CTP and MRP. Regarding cerebral flow after stenting, CCT (4.61 ± 1.6 s) was shortened, rMTT (1.12 ± 0.04) and rTTP ($r = 1.05 \pm 0.03$) decreased, and rCBF (0.91 ± 0.16) increased significantly.

Conclusion: FD-CTP provides a potentially more comprehensive hemodynamic assessment of parenchymal perfusion changes compared with QDSA during carotid stenting, but FC-CTP requires additional 18 min. FD-CTP confirmed that the normalization of cerebral hemodynamics began immediately and continued for 1−3 days.

Keywords: Carotid stenosis; Carotid stenting; Cerebral circulation time; Cerebral hemodynamic; Flat-detector; Perfusion; Quantitative digital subtraction angiography

1. Introduction

Carotid stenosis accounts for 15%−20% of all stroke incidences.[1] In the recent carotid revascularization endarterectomy versus stenting trial, carotid stenting and endarterectomy were demonstrated to have similar stroke and death rates.[2] However, carotid stenting is less invasive and

Conflicts of interest: The authors declare that they have no conflicts of interest related to the subject matter or materials discussed in this article.

* Corresponding author. Dr. Wan You Guo, Department of Radiology, Taipei Veterans General Hospital, 201, Section 2, Shi-Pai Road, Taipei 112, Taiwan, ROC.

E-mail address: wyguo@vghtpe.gov.tw (W.-Y. Guo).

https://doi.org/10.1016/j.jcma.2018.01.016

more beneficial for patients who develop carotid stenosis after irradiation for preceding head and neck cancers.[3] Hyperperfusion syndrome (HPS) is characterized by considerably increased cerebral blood flow (CBF) after successful revascularization. The clinical triad of HPS includes headache, seizure, and focal neurological deficits. The incidence of HPS ranges from 0.5% to 10%, depending on the precise definition.[4] Numerous risk factors for HPS, such as bilateral carotid stenosis, age, uncontrolled hypertension, stenotic sinus, and blood–brain barrier disruption, have been proposed in the literature; however, their exact mechanisms are not sufficiently understood.[5–8] The most widely accepted etiology involves impaired cerebral autoregulation,[9] which has been strongly correlated with impaired cerebral vasoreactivity (CVR).[9–11] CVR is evaluated through single-photon emission computed tomography (SPECT) or functional magnetic resonance (MR) imaging, and the limited availability of these evaluation approaches has restricted their application in endovascular treatment. Another alternative approach is using perfusion studies as a surrogate for CVR. By using appropriate threshold settings, studies have found increased cerebral blood volume (CBV), mean transit time (MTT), and time to peak (TTP) to be reliable predictors of HPS development after carotid revascularization.[12,13]

Early recognition of a substantial increase in CBF after stenting is crucial for preventing potentially dangerous complications through proper management by using techniques such as strict control of blood pressure, discontinuation of antiplatelet management, and administration of mannitol to control intracranial pressure.[7] Cerebral circulation time (CCT) has been used as a surrogate to monitor CBF during carotid stenting and has demonstrated considerable efficacy in detecting HPS.[14–16] The major advantage of this technique is that it rapidly provides results without requiring extra radiation and contrast. However, the overlapping vasculature in two-dimensional images limits its application in quantifying the brain parenchyma.

After an increase in the rotation speed and angle of the angiographic C-arm system, sequential CT imaging with an intravenous contrast bolus injection could successfully produce perfusion-like imaging.[17] This approach can generate reliable qualitative assessments of cerebral hemodynamics in both animal and human studies, including measurements of CBV, CBF, MTT, and TTP. The Alberta Stroke Program Early Computed Tomography (ASPECT) scores from MR perfusion (MRP) and flat-detector computed tomography perfusion (FD-CTP) in patients with acute stroke were comparable, making it possible to triage patients with large penumbral areas who could potentially benefit from endovascular therapy.[18,19] Lin et al. evaluated perfusion deficits in carotid stenosis and reported that compared with absolute quantification, the relative quantification of FD-CTP correlated more strongly with MRP.[20]

Ogasawara et al. observed immediate CBF augmentation after carotid endarterectomy.[21] However, Wilkinson et al. reported that the transit time of the first bolus remained prolonged but normalized partly 3 h after carotid stenting.[22] Soinne et al. confirmed the normalization of cerebral hemodynamics 3 days after carotid stenting.[23] The exact time sequence of perfusion changes within the 3-day period following carotid stenting remains unclear. In this study, we performed advanced FD-CTP imaging to compare the effectiveness between CCT and relative FD-CTP perfusion parameters in monitoring cerebral hemodynamics during revascularization in chronic steno-occlusive disease and to gain a better understanding of the time sequence of autoregulation after revascularization.

2. Methods

2.1. Patient selection

All patients referred to our department for carotid stenting from August 2014 to December 2015 were eligible for this study. All patients provided written informed consent after consultation. Patients who had unilateral extracranial carotid stenosis of more than 70% according to the North American Symptomatic Carotid Endarterectomy Trial criteria were eligible for inclusion. Exclusion criteria included having contralateral stenosis, poor renal or heart function, prior cerebral infarct, prior MR-evidenced territorial infarct, or being uncooperative.[24] Our local ethics committee approved this study.

2.2. Flat-detector CT perfusion

Two quantitative digital angiography and FD-CTP sessions were obtained immediately before and after stenting on the same digital subtraction angiography machine (AXIOM Artis, Siemens Healthcare, Forchheim, Germany). Fixed injection protocols and imaging acquisitions were used to obtain CCT.[25,26] Angiographic series were processed using Syngo iflow (Siemens Healthcare, Forchheim, Germany), and time–density curves were obtained for selected regions of interest (ROIs); CCT was defined as the difference in TTP between the parietal vein and the cavernous portion of the internal carotid artery (ICA) in the lateral view of a digital subtraction angiogram. CCT represents the duration required for blood to flow through the brain parenchyma. The whole FD-CTP sequence consisted of 10 C-arm rotations, and the duration was approximately 1 min. Each rotation lasted 5 s and covered 200°. The gap between the two rotations was approximately 1 s. A power injector (Liebel-Flarsheim Angiomat, Illumena) was used to administer a contrast bolus of 60 mL of Iopamiron (370 mg iodine/dL, Bracco, Italy), followed by 40 mL of normal saline at a rate of 5 mL/s through the antecubital vein. The contrast bolus commenced 5 s after the start of FD-CTP acquisition. The first two rotations were used for mask runs (clockwise and counterclockwise). The details of acquisition protocols are provided in the literature.[17,18] The datasets were sent to a workstation equipped with Syngo iflow and a prototype of DynaCT perfusion (Siemens Healthcare, Forchheim, Germany) for reconstruction. Arterial input function selection was performed on the ipsilateral

middle cerebral artery (MCA). A standard truncated singular value decomposition algorithm without delay correction was used to produce parametric color maps of CBV, CBF, TTP, and MTT.[27,28] The median interval between FD-CTP acquisitions was 37 (27–56) minutes before stent deployment and 18.3 (10.8–38) minutes after stent deployment. The overall radiation dose for a single FD-CTP was 4.6 mSv, which is comparable to a multidetector CTP dose of 3.6 mSv.[29,30]

2.3. MRP process

All MRPs were performed between the day before and after carotid stenting by using the same 1.5-T scanner (Signa HDxt, GE Healthcare, Milwaukee, USA) with an eight-channel neurovascular coil. Using an echo-planar imaging sequence, we performed 70 sequential scans for seven slices. The temporal resolution was 1 s. Imaging parameters were as follows: flip angle, 60°; TR/TE, 1000 ms/40 ms; section thickness, 7 mm (with a 7-mm imaging gap); field of view, 240 mm; and acquisition matrix, 128 × 128. A bolus injection of gadobenate dimeglumine (7 mL; Multihance, Bracco, Milan, Italy) was administered through the antecubital vein at a rate of 3 mL/s by using a power injector (Opistar Mallinckrodt Pharmaceuticals, Dublin, Ireland). The MR scan and the bolus were started simultaneously. Perfusion mismatch analyzer software (version 5.0, ASIST Group, Japan) was used for analysis.[31] The arterial input function of the ipsilateral MCA was selected in both MRP and FD-CTP. The software automatically determined the venous output function. The standard singular value decomposition method was used in the deconvolution algorithm to obtain TTP, CBV, CBF, and MTT values in both MRP and FD-CTP.

2.4. Selection of ROIs

ROIs were placed in the MCA territory at the basal ganglia level, similar to ASPECT in both stenotic and contralateral hemispheres (Fig. 1).[20,32] Two neuroradiologists who were blinded to the clinical conditions of patients manually placed the ROIs of pre- and post-stenting FD-CTPs through a side-by-side comparison. For the absolute parameter measurement, direct readouts of ROIs that were placed on pre- and post-stenting CBF, CBV, MTT, and TTP color maps in both stenotic and contralateral hemispheres were used. Those measurements were performed twice on FD-CTPs and once on MRP by each observer. For relative quantification, the ratios of hemodynamic parameters (rTTP, rCBV, rCBF, and rMTT) were defined as the readouts of ROIs in the stenotic hemisphere divided by the homologous one in the contralateral hemisphere.

2.5. Statistical analysis

SPSS software (version 20, SPSS 2010; IBM-SPSS, Chicago, IL) was used to determine the Spearman correlations of CCT, rCBF, rCBV, rMTT, and rTTP between FD-CTP and MRP before and after stenting. Peritherapeutic changes in the aforementioned parameters were compared using the Wilcoxon signed rank test. The significance level for all statistical tests was set at $p < 0.05$.

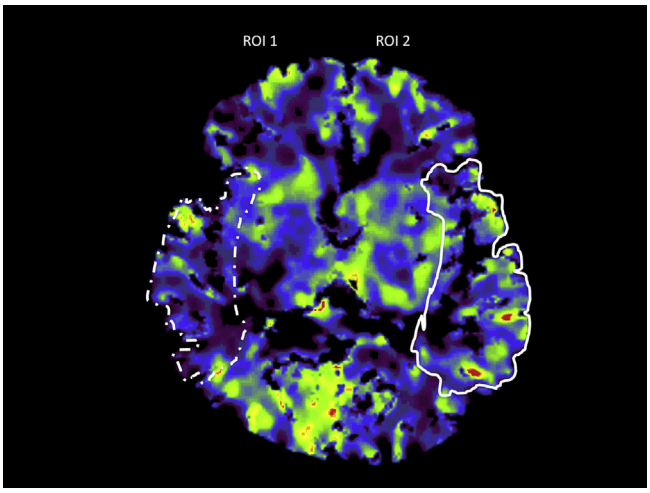

Fig. 1. Selection of ROIs in a CBV map from FD-CTP in a patient with 75% stenosis of the right ICA. ROI1 was manually drawn to include the outer middle MCA territory, posterior MCA territory, and insula according to the ASPECT scoring system. ROI2 was manually drawn to include the corresponding territory on the nonstenotic side.

3. Results

Thirty-three patients received carotid stenting. No periprocedural complications were reported. Of the 33 patients, six had contralateral stenosis, seven had a contraindication to FD-CTP due to impaired renal or heart function, and five did not receive MRP within 3 days. Moreover, two patients were uncooperative, and motion artifacts compromised their subsequent FD-CTP images. Therefore, after the exclusion of these patients, 13 patients who underwent both pre- and post-stenting FD-CTP were included (Table 1). The median age of

Table 1
Characteristics, pre- and post-stent stenosis.

NO.	Age	G	Location	Pre-D cm	Pre-S %	Post-D cm	Post-S %
1	61	M	RPICA	0.09 × 0.07	95	0.31 × 0.40	11
2	75	F	RPICA	0.14 × 0.26	86	0.38 × 0.40	44
3	57	M	RDCCA	0.14 × 0.12	94	0.38 × 0.41	44
4	45	F	LPICA	029 × 0.28	77	0.57 × 0.51	12
5	73	F	LPICA	0.25 × 0.44	75	0.38 × 0.40	66
6	61	F	RPICA	0.26 × 0.21	80	0.40 × 0.39	61
7	91	M	LPICA	0.19 × 0.31	85	0.46 × 0.48	20
8	66	F	LPICA	0.15 × 0.16	85	0.27 × 0.27	61
9	74	M	RPICA	0.17 × 0.01	99	0.21 × 0.23	65
10	61	M	LPICA	0.09 × 0.15	95	0.45 × 0.36	45
11	62	M	LPICA	0.07 × 0.12	97	0.38 × 0.43	53
12	78	F	LDCCA	0.21 × 0.80	93	0.36 × 0.41	41
13	69	M	RPICA	0.15 × 0.15	84	0.33 × 0.28	66

RPICA = Right proximal internal cerebral artery; LPICA = Left proximal internal cerebral artery.
RDCCA = Right distal common carotid artery; LDCCA = Left distal common carotid artery.
Pre-S %: Percentage of stenosis before stenting.
Post-S %: Percentage of stenosis after stenting.

the 13 patients was 71 years, ranging from 43 to 88 years; seven patients were men and six patients were women. The median stenosis degree was 86% (75%–99%). No significant stenosis after stenting was noted in all patients. All patients had satisfactory angiographic collaterals, according to the classification by Henderson et al.[33] Five patients had previously received radiotherapy for cancers of the head and neck without contralateral stenosis. The intraclass correlation coefficients for the two readers were between 0.71 and 0.91. The intraobserver kappa values for readers A and B ranged from 0.75 to 0.99 and from 0.75 to 0.98, respectively (Table 2). The absolute value of the parameters were not correlation between FD-CTP and MRP (Table 2). However, before stenting, rCBF ($r = 0.73$) and rTTP ($r = 0.58$) were moderately-to-strongly correlated between FD-CTP and MRP (Fig. 2). The CCT exhibited a weak, moderate, and strong correlation with rCBF ($r = -0.34$), rTTP ($r = 0.45$), and rMTT ($r = 0.69$). respectively, in MRP (Fig. 3). After stenting, none of the parameters were correlated between FD-CTP and MRP (see Table 3).

For peritherapeutic measurements, both MRP and FD-CTP exhibited the same trends: rCBF increased, rMTT decreased, and rTTP decreased significantly, but rCBV did not exhibit a significant peritherapeutical change. The observed CCT was shortened significantly from 4.5 ± 1.5 to 3.9 ± 1.0 s after stenting (Table 4).

4. Discussion

Compared with CCT parameters, the hemodynamic parameters in FD-CTP were more strongly correlated with the corresponding parameters in MRP. This is because the correspondence of ROIs in three dimensions between FD-CTP and MRP can improve the accuracy level. Additionally, the waveforms of the time–density curves of the intravenous injection were more comparable in FD-CTP and MRP examinations, whereas the waveform of the time–density curve of the intra-arterial injection used in the digital subtraction angiography for CCT might be somewhat altered, as described in the literature.[34] Previous studies have reported strong correlations between CCT and rCBF, rMTT, and rTTP.[14,15] Nevertheless, CCT was correlated with only time-dependent parameters (rMTT and rTTP) in MRP in our study. TTP was directly estimated on the basis of a gamma-variate-fitted time–density curve from the voxel of interest in FD-CTP, and it was less sensitive to deconvolution algorithms than other perfusion parameters. Similar to MTT, CCT was used to quantify the time required for blood to flow through the brain parenchyma in angiography; therefore, both parameters were strongly correlated.

The temporal resolution of FD-CTP acquisition used in this study was approximately 6 s, which is longer than the MRP scan interval. Hirata et al. reported that CBF and CBV remained almost unchanged when the scan interval was less than 5 and 10 s, respectively; however, MTT may be underestimated when the scan interval exceeds 2 s.[35] The moderate correlation of rCBF and rMTT between FD-CTP and MRP in our study evinces the feasibility of obtaining reliable relative perfusion parameters with a 6-s interval. We observed only one case of excessive MTT. Because the same deconvolution algorithm was used in FD-CTP and MRP with high consistency in CBF (another parameter after deconvolution), deconvolution may not have been the cause of the error.[36] This outlier in MTT may be caused by factors such as a prolonged scan interval, the waveform of the time–density curve, or a reconstruction artifact.[37,38] The continuation of autoregulation after stenting between the timing of FD-CTP and MRP might explain the lack of correlation between the two studies.

rCBF, rMTT, and rTTP with both MRP and FD-CTP exhibited results similar to those reported in the literature: restoration of CBF and shortened stenotic-side MTT and TTP after revascularization (Fig. 4).[39,40] As reported in a previous study, increased rCBV and prolonged MTT and TTP before stenting are predictors of poor CVR and are associated with a predisposition to HPS in perfusion studies.[41] CVR was not sensitive to hemodynamic changes during stenting due to individual CVR variations. CVR indicates the vasodilatation of the microvasculature and the recruitment of collateral circulation distal to the site of a severe stenosis in response to ischemia.[42–44] Overall, the average severity of the stenosis degree (83%) in our study was not severe enough to cause any distal vasodilatation, collaterals, or a subsequent increase in CBV compared with the contralateral side. Therefore, peritherapeutic CBV did not change significantly. This finding explains why HPS was not observed in our patient population.

Fukuda et al. reported that increased CBF was observed immediately after carotid endarterectomy through SPECT, constituting the fastest follow-up interval of all imaging modalities after carotid revascularization.[45] The earliest observation of dynamic susceptibility of MRP was conducted 3 h after stenting in a small patient population: Wilkinson et al. observed that the asymmetry of rCBV decreased 3 h after stenting, but this change did not reach statistical significance.[22] Other studies with later follow-up intervals have also reported similar trends.[23,44] In contrast to most other studies,

Table 2
Intraobserver and interobserver variabilities of FD-CTP in absolute and relative CBF, CBV, MTT, and TTP.

Absolute	Reader A	Read B	Inter-observer
	kappa (CI)	kappa (CI)	kappa (CI)
CBF (ml/100 g/min)	0.87 (0.82–0.92)[a]	0.85 (0.80–0.91)[a]	0.73 (0.68–0.78)[a]
CBV (ml/100 g)	0.89 (0.84–0.94)[a]	0.91 (0.87–0.93)[a]	0.86 (0.81–0.891[a]
MTT (seconds)	0.75 (0.69–0.80)[a]	0.75 (0.71–0.79)[a]	0.73 (0.68–0.78)[a]
TTP (seconds)	0.80 (0.75–0.85)[a]	0.79 (0.84–0.84)[a]	0.71 (0.66–0.76)[a]
Relative			
rCBF (ml/100 g/min)	0.95 (0.99–0.94)[a]	0.96 (0.99–0.93)[a]	0.84 (0.89–0.79)[a]
rCBV (ml/100 g)	0.99 (0.98–0.99)[a]	0.98 (0.99–0.95)[a]	0.93 (0.96–0.89)[a]
rMTT (seconds)	0.87 (0.91–0.82)[a]	0.93 (0.88–0.96)[a]	0.81 (0.86–0.75)[a]
rTTP (seconds)	0.91 (0.94–0.86)[a]	0.90 (0.94–0.85)[a]	0.91 (0.94–0.86)[a]

CI = confidence interval; CBF = cerebral blood flow; CBV = cerebral blood volume; FD-CTP = flat-detector CT perfusion; MTT = mean transit time; TTP = time to peak.
[a] Indicates a significant difference.

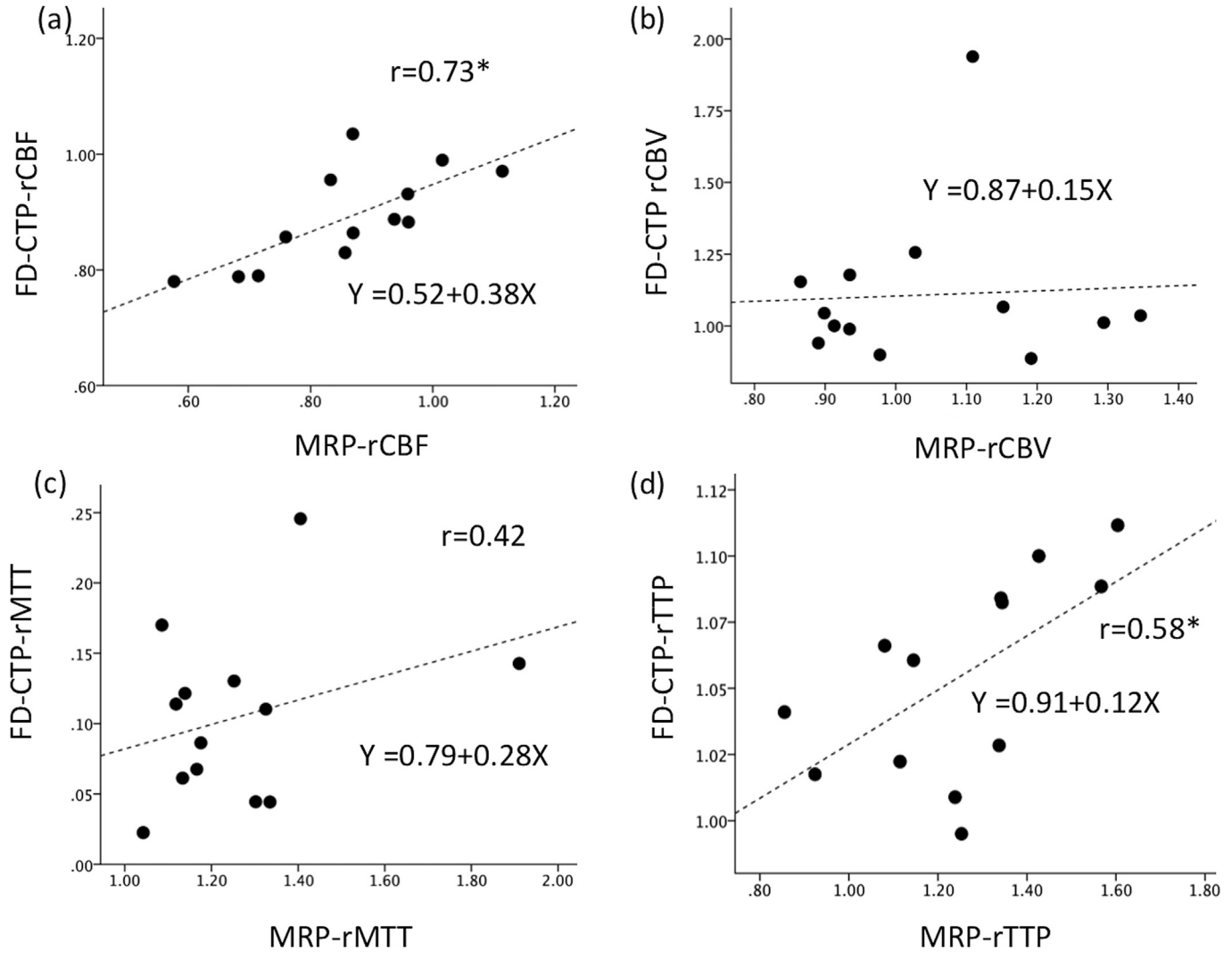

Fig. 2. Correlation between (a) rCBF, (b) rCBV, (c) rMTT, and (d) rTTP in MRP and FD-CTP.

Pinero et al. revealed that none of the parameters in susceptibility of MRP demonstrated significant restoration of perfusion 1 day after stenting. However, the follow-up observation in the same study showed that TTP significantly decreased 1 month after stenting.[46] By contrast, Soinne et al. reported that cerebral perfusion improved 3 days after stenting, but only MTT was significantly normalized, and this benefit persisted beyond 30 days.[23]

In our FD-CTP study, we observed that the normalization of cerebral hemodynamics had already occurred between 10 and 30 min after stenting. The variability of normalization is likely due to covariates such as the preexisting cerebrovascular reservoir and the connectivity of the circle of Willis.[47] We also observed excessive cerebral flow augmentation (rCBF = 1.07, overshoot phenomenon) between 10 and 30 min after carotid stenting. Restoration of blood flow rebounded immediately to its highest amplitude after stenting and gradually normalized after 30 days.[23,44] In the literature, a 100% increase in CBF in MRP or a 45% increase in CBV in cone-beam CT are two signs of hyperperfusion.[41] In our study, no patients satisfied the aforementioned two criteria or developed hyperperfusion.

Our study has several limitations. First, our sample size was small; therefore, additional studies with a larger sample size are warranted to confirm our results. The use of multidetector CTP for measurement validation would be a more effective approach; however, iodine contrast-induced nephrotoxicity is always a major concern, especially in elderly patients.[48] Each FD-CTP imaging dataset was reconstructed through a 5-s C-arm rotation. We expect that the rotation time would decrease in newer imaging systems. Two patients were initially enrolled but later excluded because motion artifacts compromised the imaging process. The reconstruction of the imaging dataset by averaging 5-s acquisitions is vulnerable to motion artifacts. This drawback potentially limits its application in uncooperative patients.

The exclusive availability of FD-CTP in the angiosuite indicates that territorial quantitative cerebral hemodynamic evaluation is feasible and can potentially facilitate improved

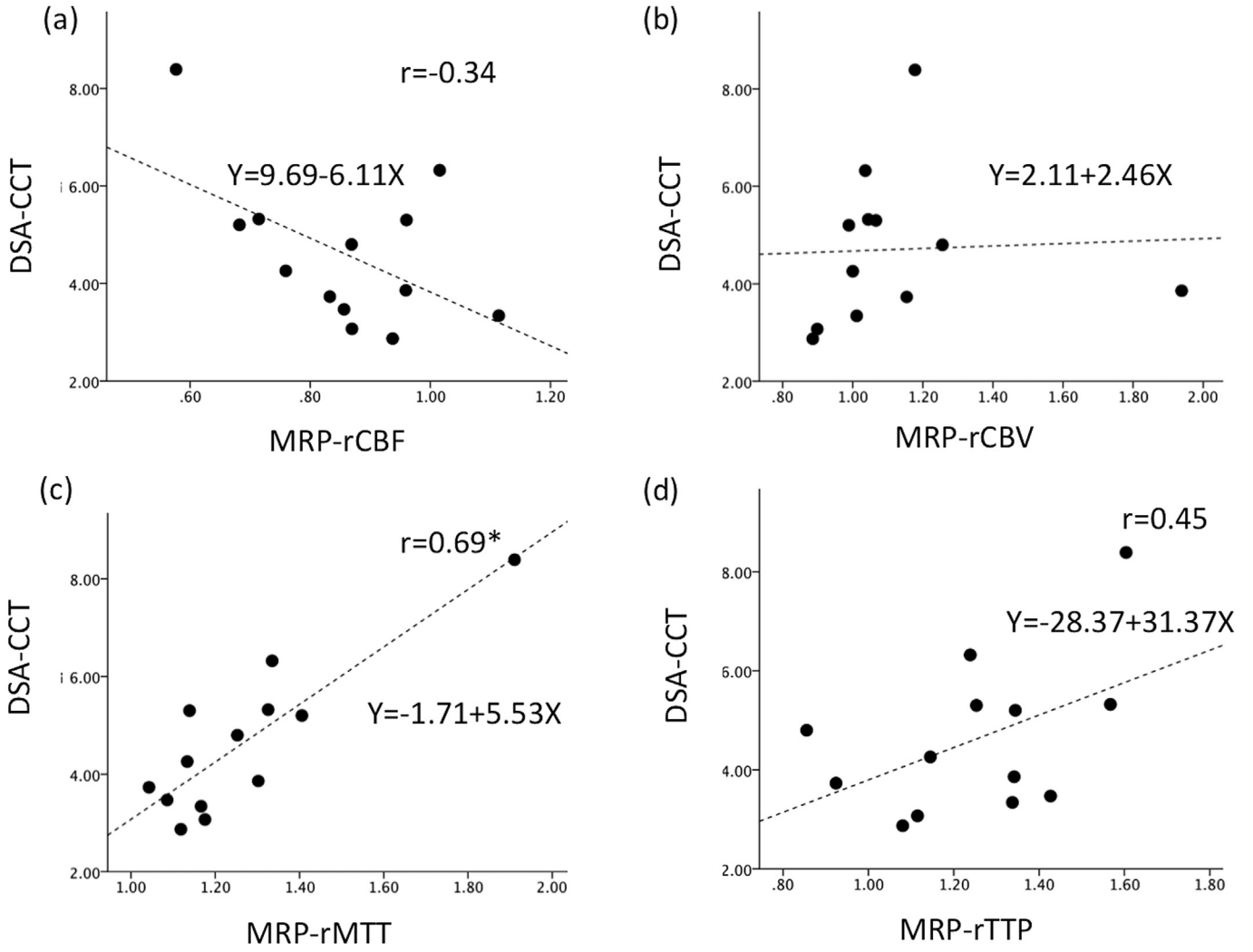

Fig. 3. Correlation between CCT and (a) rCBF, (b) rCBV, (c) rMTT, and (d) rTTP in MRP.

imaging workflow for patients with acute stroke inside the angiosuite.[18] Furthermore, FD-CTP revealed that the normalization of cerebral hemodynamics occurred between 10 and 30 min after stenting. Although rCBF showed the strongest correlation between MRP and FD-CTP in both pre- and post-stenting evaluations, the visual perception of improved MTT and TTP peritherapeutically was better than that of CBF.[38] By using these parameters, we can more accurately assess the flow changes peritherapeutically compared with CCT alone to improve patient safety.

Table 3
Comparisons of TTP, CBV, CBF and MTT in ipsilateral and contralateral hemispheres before and after carotid stenting.

Stenotic side	Before		After		*p*
	Median	(Q1–Q3)	Median	(Q1–Q3)	
CBF (ml/100 g/min)	38	(25–57)	41.5	(26–62)	0.061
CBV (ml/100 g)	40	(3.4–4.8)	51	(3.1–8.1)	0.064
MTT (seconds)	10.1	(6.9–15.9)	9.2	(6.8–14.2)	0.12
TTP (seconds)	16.7	(11.7–19.4)	12.9	(12.3–17.8)	0.08
Contralateral side	Median	(Q1–Q3)	Median	(Q1–Q3)	
CBF (ml/100 g/min)	40.5	(24–52)	45	(26–64)	0.144
CBV (ml/100 g)	4.5	(3.1–6.0)	5.5	(3.2–8.3)	0.068
MTT (seconds)	8.6	(7.8–13.0)	8.25	(7.3–15.5)	0.91
TTP (seconds)	16.7	(11.5–18.7)	12.9	(12.3–18.5)	0.43

Q1: first quartile; Q3: third quartile.

Table 4
Comparisons of CCT, rTTP, rCBV, rCBF, and rMTT in MRP and FD-CTP before and after carotid stenting.

	Before	After	*p*
	Median (Q1–Q3)	Median (Q1–Q3)	
CCT (seconds)	4.5 (3.5–5.3)	3.9 (3.4–3.8)	0.043[a]
MRP			
rCBF	0.86 (0.75–0.95)	1.02 (0.87–1.03)	0.007[a]
rCBV	0.97 (0.91–1.15)	0.96 (0.92–1.08)	0.833
rMTT	1.17 (1.13–1.32)	0.95 (0.90–1.06)	0.002[a]
rTTP	1.25 (1.11–1.34)	0.97 (0.83–1.08)	<0.001
FD-CTP			
rCBF	0.87 (0.79–0.95)	1.07 (1.02–1.19)	0.043[a]
rCBV	1.01 (0.95–1.06)	0.98 (0.92–1.12)	0.445
rMTT	1.11 (1.06–1.13)	0.89 (0.81–0.91)	0.02[a]
rTTP	1.05 (1.02–1.08)	1.01 (0.95–1.03)	<0.001[a]

Q1: first quartile; Q3: third quartile.
[a] Indicates a significant difference.

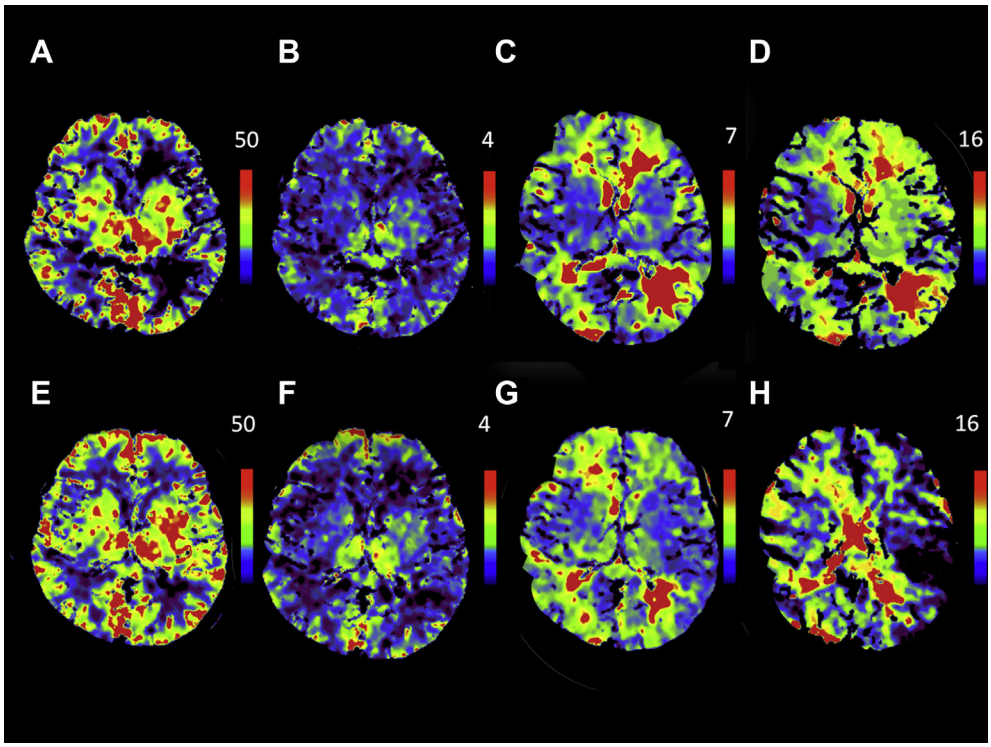

Fig. 4. A 61-year-old man with left ICA stenosis of 90% received carotid stenting. FD-CTP before stenting **(A: CBF, B: CBV; C: MTT; D: TTP)** and after stenting **(E: CBF, F: CBV; G: MTT; H: TTP)** was performed. Increased CBF and CBV in the left MCA territory after stenting were noted. A decrease in MTT in the left MCA territory was also noted. TTP was considerably reduced.

In conclusion, compared with CCT, the hemispheric relative quantification of FD-CTP was proven to provide robust quantitative assessments of cerebral hemodynamic changes inside the angiosuite. Restoration with slight cerebral blood overflow and the normalization of MTT and TTP occurred almost immediately after carotid stenting. The results obtained from FD-CTP within the angiosuite enable us to better understand the pathophysiology of HPS, and it can potentially play a role in identifying patients at a high risk of hyperperfusion, thus possibly improving patient safety.

Acknowledgments

This research was co-sponsored by two grants: 1) the Taipei Veterans General Hospital and Siemens Healthcare (grant number: T1100200) and 2) the Taipei Veterans General Hospital (grant number: V105C-145).This manuscript was edited by Wallace Academic Editing.

References

1. Chimowitz MI, Lynn MJ, Derdeyn CP, Turan TN, Fiorella D, Lane BF, et al. Stenting versus aggressive medical therapy for intracranial arterial stenosis. *N Eng J Med* 2011;**365**:993–1003.
2. Brott TG, Hobson RWI, Howard G, Roubin GS, Clark WM, Brooks W, et al. Stenting versus endarterectomy for treatment of carotid-artery stenosis. *N Eng J Med* 2010;**363**:11–23.
3. Chang YJ, Chang TC, Lee TH, Ryu SJ. Predictors of carotid artery stenosis after radiotherapy for head and neck cancers. *J Vasc Surg* 2009;**50**:280–5.
4. Moulakakis KG, Mylonas SN, Sfyroeras GS, Andrikopoulos V. Hyperperfusion syndrome after carotid revascularization. *J Vasc Surg* 2009;**49**:1060–8.
5. Ivens S, Gabriel S, Greenberg G, Friedman A, Shelef I. Blood-brain barrier breakdown as a novel mechanism underlying cerebral hyperperfusion syndrome. *J Neurol* 2010;**257**:615–20.
6. Ascher E, Markevich N, Schutzer RW, Kallakuri S, Jacob T, Hingorani AP. Cerebral hyperperfusion syndrome after carotid endarterectomy: predictive factors and hemodynamic changes. *J Vasc Surg* 2003;**37**:769–77.
7. Abou-Chebl A, Bajzer CT, Krieger DW, Furlan AJ, Yadav JS. Multimodal therapy for the treatment of severe ischemic stroke combining GPIIb/IIIa antagonists and angioplasty after failure of thrombolysis. *Stroke* 2005;**36**:2286–8.
8. Lin CJ, Chang FC, Tsai FY, Guo WY, Hung SC, Chen DY, et al. Stenotic transverse sinus predisposes to poststenting hyperperfusion syndrome as evidenced by quantitative analysis of peritherapeutic cerebral circulation time. *AJNR Am J Neuroradiol* 2014;**35**:1132–6.
9. Hosoda K, Kawaguchi T, Shibata Y, Kamei M, Kidoguchi K, Koyama J, et al. Cerebral vasoreactivity and internal carotid artery flow help to identify patients at risk for hyperperfusion after carotid endarterectomy. *Stroke* 2001;**32**:1567–73.
10. Iwata T, Mori T, Tajiri H, Nakazaki M. Predictors of hyperperfusion syndrome before and immediately after carotid artery stenting in single-photon emission computed tomography and transcranial color-coded real-time sonography studies. *Neurosurgery* 2011;**68**:649–55.
11. Chang TY, Liu HL, Lee TH, Kuan WC, Chang CH, Wu HC, et al. Change in cerebral perfusion after carotid angioplasty with stenting is related to cerebral vasoreactivity: a study using dynamic susceptibility-weighted contrast-enhanced MR imaging and functional MR imaging with a breath-holding paradigm. *AJNR Am J Neuroradiol* 2009;**30**:1330–6.
12. Tseng YC, Hsu HL, Lee TH, Hsieh IC, Chen CJ. Prediction of cerebral hyperperfusion syndrome after carotid stenting: a cerebral perfusion computed tomography study. *J Comput Assist Tomogr* 2009;**33**:540–5.

13. Chang CH, Chang TY, Chang YJ, Huang KL, Chin SC, Ryu SJ, et al. The role of perfusion computed tomography in the prediction of cerebral hyperperfusion syndrome. *PLoS One* 2011;**6**:e19886.
14. Lin CJ, Hung SC, Chang FC, Guo WY, Luo CB, Kowarschik M, et al. Finding the optimal deconvolution algorithm for MR perfusion in carotid stenosis: correlations with angiographic cerebral circulation time. *J Neuroradiol* 2016;**43**:290−6.
15. Narita S, Aikawa H, Nagata S, Tsutsumi M, Nii K, Yoshida H, et al. Intraprocedural prediction of hemorrhagic cerebral hyperperfusion syndrome after carotid artery stenting. *J Stroke Cerebrovasc Dis* 2013;**22**: 615−9.
16. Aikawa H, Kazekawa K, Tsutsumi M, Onizuka M, Iko M, Kodama T, et al. Intraprocedural changes in angiographic cerebral circulation time predict cerebral blood flow after carotid artery stenting. *Neurol Med Chir (Tokyo)* 2010;**50**:269−74.
17. Royalty K, Manhart M, Pulfer K, Deuerling-Zheng Y, Strother C, Fieselmann A, et al. C-arm CT measurement of cerebral blood volume and cerebral blood flow using a novel high-speed acquisition and a single intravenous contrast injection. *AJNR Am J Neuroradiol* 2013;**34**:2131−8.
18. Struffert T, Deuerling-Zheng Y, Kloska S, Engelhorn T, Lang S, Mennecke A, et al. Dynamic angiography and perfusion imaging using flat detector CT in the angiography suite: a pilot study in patients with acute middle cerebral artery occlusions. *AJNR Am J Neuroradiol* 2015;**36**: 1964−70.
19. Goyal M, Demchuk AM, Menon BK, Eesa M, Rempel JL, Thornton J, et al. Randomized assessment of rapid endovascular treatment of ischemic stroke. *N Engl J Med* 2015;**372**:1019−30.
20. Lin CJ, Guo WY, Chang FC, Hung SC, Chen KK, Yu DZ, et al. Using flat-panel perfusion imaging to measure cerebral hemodynamics: a pilot feasibility study in patients with carotid stenosis. *Medicine (Baltimore)* 2016;**95**:e3529.
21. Ogasawara K, Sakai N, Kuroiwa T, Hosoda K, Iihara K, Toyoda K, et al. Intracranial hemorrhage associated with cerebral hyperperfusion syndrome following carotid endarterectomy and carotid artery stenting: retrospective review of 4494 patients. *J Neurosurg* 2007;**107**:1130−6.
22. Wilkinson ID, Griffiths PD, Hoggard N, Cleveland TJ, Gaines PA, Macdonald S, et al. Short-term changes in cerebral microhemodynamics after carotid stenting. *AJNR Am J Neuroradiol* 2003;**24**:1501−7.
23. Soinne L, Helenius J, Tatlisumak T, Saimanen E, Salonen O, Lindsberg PJ, et al. Cerebral hemodynamics in asymptomatic and symptomatic patients with high-grade carotid stenosis undergoing carotid endarterectomy. *Stroke* 2003;**34**:1655−61.
24. Barnett HJM, Taylor DW, Haynes RB, Sackett DL, Peerless SJ, Ferguson GG, et al. Beneficial effect of carotid endarterectomy in symptomatic patients with high-grade carotid stenosis. *N Engl J Med* 1991;**325**:445−53.
25. Lin CJ, Chang FC, Guo WY, Hung SC, Luo CB, Beilner J, et al. Changes of time-attenuation curve blood flow parameters in patients with and without carotid stenosis. *AJNR Am J Neuroradiol* 2015;**36**:1176−81.
26. Lin CJ, Hung SC, Guo WY, Chang FC, Luo CB, Beilner J, et al. Monitoring peri-therapeutic cerebral circulation time: a feasibility study using color-coded quantitative DSA in patients with steno-occlusive arterial disease. *AJNR Am J Neuroradiol* 2012;**33**:1685−90.
27. Fieselmann A, Kowarschik M, Ganguly A, Hornegger J, Fahrig R. Deconvolution-based CT and MR brain perfusion measurement: theoretical model revisited and practical implementation details. *Int J Biomed Imaging* 2011;**2011**:467563.
28. Ganguly A, Fieselmann A, Marks M, Rosenberg J, Boese J, Deuerling-Zheng Y, et al. Cerebral CT perfusion using an interventional C-arm imaging system: cerebral blood flow measurements. *AJNR Am J Neuroradiol* 2011;**32**:1525−31.
29. Wu TH, Hung SC, Sun JY, Lin CJ, Lin CH, Chiu CF, et al. How far can the radiation dose be lowered in head CT with iterative reconstruction? Analysis of imaging quality and diagnostic accuracy. *Eur Radiol* 2013;**23**:2612−21.
30. Smith AB, Dillon WP, Lau BC, Gould R, Verdun FR, Lopez EB, et al. Radiation dose reduction strategy for CT protocols: successful implementation in neuroradiology section. *Radiology* 2008;**247**:499−506.
31. Kudo K, Sasaki M, Ogasawara K, Terae S, Ehara S, Shirato H. Difference in tracer delay-induced effect among deconvolution algorithms in CT perfusion analysis: quantitative evaluation with digital phantoms. *Radiology* 2009;**251**:241−9.
32. Pexman JH, Barber PA, Hill MD, Sevick RJ, Demchuk AM, Hudon ME, et al. Use of the Alberta stroke program early CT score (ASPECTS) for assessing CT scans in patients with acute stroke. *AJNR Am J Neuroradiol* 2001;**22**:1534−42.
33. Henderson RD, Eliasziw M, Fox AJ, Rothwell PM, Barnett HJ. Angiographically defined collateral circulation and risk of stroke in patients with severe carotid artery stenosis. North American Symptomatic Carotid Endarterectomy Trial (NASCET) Group. *Stroke* 2000;**31**: 128−32.
34. Lin CF, Hsu SP, Lin CJ, Guo WY, Liao CH, Chu WF, et al. Prolonged cerebral circulation time is the best parameter for predicting vasospasm during initial CT perfusion in subarachnoid hemorrhagic patients. *PLoS One* 2016;**11**:e0151772.
35. Hirata M, Murase K, Sugawara Y, Nanjo T, Mochizuki T. A method for reducing radiation dose in cerebral CT perfusion study with variable scan schedule. *Radiat Med* 2005;**23**:162−9.
36. Ibaraki M, Ohmura T, Matsubara K, Kinoshita T. Reliability of CT perfusion-derived CBF in relation to hemodynamic compromise in patients with cerebrovascular steno-occlusive disease: a comparative study with 15O PET. *J Cereb Blood Flow Metab* 2015;**35**:1280−8.
37. Fieselmann A, Ganguly A, Deuerling-Zheng Y, Zellerhoff M, Rohkohl C, Boese J, et al. Interventional 4-D C-arm CT perfusion imaging using interleaved scanning and partial reconstruction interpolation. *IEEE Trans Med Imaging* 2012;**31**:892−906.
38. Manhart MT, Kowarschik M, Fieselmann A, Deuerling-Zheng Y, Royalty K, Maier AK, et al. Dynamic iterative reconstruction for interventional 4-D C-arm CT perfusion imaging. *IEEE Trans Med Imaging* 2013;**32**:1336−48.
39. Tavares A, Caldas JG, Castro CC, Puglia Jr P, Frudit ME, Barbosa LA. Changes in perfusion-weighted magnetic resonance imaging after carotid angioplasty with stent. *Interv Neuroradiol* 2010;**16**:161−9.
40. Szarmach A, Halena G, Buczny J, Studniarek M, Markiet K, Szurowska E, et al. Evaluation of changes in the parameters of brain tissue perfusion in multi-slice computed tomography in patients after carotid artery stenting. *Pol J Radiol* 2011;**76**:7−15.
41. Fujimoto M, Itokawa H, Moriya M, Okamoto N, Sasanuma J. Evaluation of Cerebral Hyperperfusion After Carotid Artery Stenting Using CArm CT Measurements of Cerebral Blood Volume. *Clin Neuroradiol* 2018;**28**: 253−60.
42. Powers WJ. Cerebral hemodynamics in ischemic cerebrovascular disease. *Ann Neurol* 1991;**29**:231−40.
43. Doerfler A, Eckstein HH, Eichbaum M, Heiland S, Benner T, Allenberg JR, et al. Perfusion-weighted magnetic resonance imaging in patients with carotid artery disease before and after carotid endarterectomy. *J Vasc Surg* 2001;**34**:587−93.
44. Yang B, Chen W, Yang Y, Lin Y, Duan Y, Li J, et al. Short- and long-term hemodynamic and clinical effects of carotid artery stenting. *AJNR Am J Neuroradiol* 2012;**33**:1170−6.
45. Fukuda T, Ogasawara K, Kobayashi M, Komoribayashi N, Endo H, Inoue T, et al. Prediction of cerebral hyperperfusion after carotid endarterectomy using cerebral blood volume measured by perfusion-weighted MR imaging compared with single-photon emission CT. *AJNR Am J Neuroradiol* 2007;**28**:737−42.
46. Pinero P, Gonzalez A, Moniche F, Martinez E, Cayuela A, Gonzalez-Marcos JR, et al. Progressive changes in cerebral perfusion after carotid stenting: a dynamic susceptibility contrast perfusion weighted imaging study. *J Neurointerv Surg* 2014;**6**:527−32.
47. Jongen LM, van der Worp HB, Waaijer A, van der Graaf Y, Mali WP. Interrelation between the degree of carotid stenosis, collateral circulation and cerebral perfusion. *Cerebrovasc Dis* 2010;**30**:277−84.
48. Rosovsky M, Rusinek H. Dose-related nephrotoxicity. *Radiology* 2006; **240**:614.